23rd IMEKO TC4 International Symposium
Electrical & Electronic Measurements Promote Industry 4.0
September 17-20, 2019，Xi'an, China

Discussion of Power Quality Metrics suitable for DC Power Distribution and Smart Grids

Andrea Mariscotti

ASTM Sagl, Chiasso, Switzerland, andrea.mariscotti@astm-e.ch

***Abstract* – PQ metrics for DC distribution systems are considered and reviewed with the objective of covering typical PQ phenomena, of finding similarity with the more proven indexes for AC systems, identifying the most promising approaches. Both time and frequency domain methods are considered, with emphasis on compact implementation and immediacy of output quantities. Behaviour and performance are verified against a first set of data representing the line voltage of a DC 3 kV railway system.**

***Keywords* – Power Quality, DC distribution network, DC smart grid.**

I. INTRODUCTION

There is a widespread use of DC distribution networks at various voltage levels: electrified transportation systems (railways, metros, tram lines including various energy storage devices, wayside and on-board), power generation and interconnection of various and different power sources (photovoltaic systems, micro-turbines, wind farms, etc.), supply of wide data centres, including energy backup facilities (such as super-capacitors and batteries).

Power Quality indices are well documented for AC networks and systems with abundance of standards and literature [1]-[4], useful as input for the forthcoming discussion on PQ DC metrics. Conversely, DC distribution is still not satisfactorily and comprehensively covered in terms of studies [5]-[9] and standards [10], and conditioned by definitions for AC systems [11][12].

The relevance of a comprehensive and adequate definition of PQ indices for DC distribution is both metrological and regulatory, considering the widespread use of DC distribution, the increasing figures for the load and generation power, the Switched-Mode Power Supplies emissions featuring increased switching frequency and diversified modulations [13], the possible issues related to electric interfaces and new customers, as well as the fair and accurate billing of energy consumption.

II. DC PQ METRICS

PQ indexes may be based on time- or frequency-domain quantities, with preference for the latter to preserve similarity with AC PQ indexes. Harmonics and inter-harmonics have received much attention, as well as methods for signal representation, the most popular being Fourier-based spectral representations, although various wavelet-like kernels have been extensively considered to widen the range of covered phenomena (non-stationary harmonics and inter-harmonics, unbalances, sags, etc.) and to ensure fast reaction times and adaptability of PQ algorithms [14]-[16]. The scenario is simplified for DC systems, where both fundamental frequency and phase unbalance are, let us say, unknown phenomena. However, lacking a unique fundamental may cause problems of spectral leakage and synchronous sampling.

The reduced size of loads and generation connected to DC smart grids, compared to AC medium- and high-voltage distribution networks, is accompanied by smarter switching and distortion compensation techniques, bringing the residual disturbance to a higher frequency range. It is thus commonplace that DC/DC converters operates in the tens to hundreds kHz with emissions thus well above the interval where harmonics are recognized, also from a regulatory point of view [17]. A DC network with several connected Switched-Mode Power Supplies (SMPS) is thus populated by various different un-synchronized switching fundamentals, each related to the commutation of a converter module.

Several exigencies play in favor of a definition of time-domain PQ indexes (or "mixed domain", possibly with advanced methods such as wavelets): lack of fundamental and, as such, of harmonics; the concept of ripple visualized as the excursion of the measured signal over an ideally flat steady state dc component; inclusion of high-frequency phenomena without the computational burden of a full DFT; tracking signal discontinuities and transients distinguishing them from (quasi) steady components.

A. Low Frequency Sinusoidal Distortion (LFSD)

It is a frequency domain index based on a simple rms concept, and thus a direct translation of THD indices [5]:

$$D_{LFSD} = \left[\sum_{k>0}^{k_{max}} (Q[k]/Q[0])^2 \right]^{1/2} \quad (1)$$

where: $Q[0]$ is the dc value; $Q[k]$ is the frequency spectrum of $q[n]$ (rms); k is the frequency index between 0 and $k_{max}=F_{max}/df$, with df the frequency resolution.

A more general formulation is attainable if the term $Q[0]$ is transformed into a general estimate of the steady

state, or the nominal, DC voltage, but unrelated from the calculation of the Q vector by means of DFT.

B. Waveform Distortion Ratio (WDR)

Quite a general index for ac systems is described in [16]: the Waveform Distortion Ratio (WDR).

$$WDR = \frac{\sqrt{|V_{m1} - V_1|^2 + \sum_{i=2}^{M} (V_{\text{harm},i})^2 + \sum_{i=1}^{N} (V_{\text{inth},i})^2}}{V_1} \quad (2)$$

where (from the original formulation): V_1 is the rated and V_{m1} is the measured fundamental amplitude; $V_{\text{harm},i}$ and $V_{\text{inth},i}$ are the i-th harmonic and inter-harmonic up to a maximum number M and N, respectively.

When transferred to the DC case, V_1 is then referred to the DC nominal value and V_{m1} is a steady state value (or mean value) estimated on a suitable time interval. Recalling definitions in MIL-STD-704 [10] such a steady state value may be estimated with a 1 s time window. For DC systems there is no real distinction between harmonics and inter-harmonics (unless "harmonic" defines network component related to the rectifying process and related to the fundamental of the ac feeding line).

After applying these changes and compacting the original *WDR* formulation, it shows as equivalent to D_{LFSD}, losing the concept of harmonic and selecting for the calculation a given number of the largest components, analogous to the calculation of SA and SAP below.

C. SA and SAP ripple indexes

These ripple indexes are calculated using the sum of the spectral components and not their square, thus in relationship to the concept of ripple rather than to that of rms or distortion [6]-[8]. The spectrum $Q[k]$ is computed on a $T = 1$ s time window (again in compliance with the direction set forth in the MIL-STD-704).

The ripple index is thus calculated as the summation of the components above a given threshold *thr*, identified by the set K_{thr}. Two indexes were considered in [6]: Sum-of-Amplitudes (SA) and Sum-of-Amplitudes-and-Phases (SAP). The reason is that the latter better follows signal variations and is able to quantify ripple as it occurs by time-domain superposition of different ac components, at the expense of a doubled computational effort.

$$q_{DFT,T,SA} = \sum_{k \in K_{thr}} |Q[k]| \quad q_{DFT,T,SAP} = \sum_{k \in K_{thr}} Q[k] \quad (3)$$

The *thr* value must be carefully chosen non to leave out any significant component, but to keep at the same time the size of K_{thr} as low as possible: values between 0.1% and 1% are suitable with the smallest value including in general all spectral components but leaving out the largest part of noise (justified on the ground of an assumed approximate 60 dB signal-to-noise ratio and the 10^{-5} and 10^{-6} thresholds tested in [6]). Additionally, to avoid the proliferation of spectral lines due to the finer frequency resolution when selecting longer time windows, peak detection should be performed, simply by isolating the largest peak of each spectral neighbourhood, a symmetric interval $\pm\delta f$ around each central frequency component. It is remarked that suppression of noise floor is almost always necessary not to falsely bias the results.

D. Time-domain peak-to-peak ripple

More than a PQ index, it is the definition itself of ripple. The value q_{pp} of the $q[n]$ sequence over k_T samples interval (k_T given by the selected minimum time window T) was originally expressed as:

$$q_{pp,T} = \max_{n,k} \{q[n] - q[n + k + k_T]\} \quad (4)$$

where max{ } operation is done over admissible values of n and k, positive integers, so that the two terms between curly braces cannot be "closer" than k_T samples.

By separating n and k (left as index of the time window interval) and expressing differently the minimum time difference and the observation window length (for clarity) the following expression may be derived, where the quantity $q_{pp}[n]$ is now calculated at each time step:

$$q_{pp,T} = \max_{n} \{|q_{pp}[n]|\} \quad (5a)$$

$$q_{pp}[n] = \max_{k \in [k_1:k_2]} \{|q[n] - q[n+k]|\} \quad (5b)$$

with k_1 and k_2 indicating the extremes of an interval that is defined as the minimum time difference T_{min} and the observation window length T, namely $k_1 = T_{min}/t_s$, $k_2 = T/t_s$.

For comparison with the other indexes, the peak-to-peak ripple shall be divided by 2, to express a peak value.

E. Percentiles

An approach based on percentiles of the signal values was proposed in [9]: distance and ratio between two percentiles are calculated for a given threshold y% and its complement to 100 (100-y%). The y-th percentile variation is expressed as the difference of two plus and minus percentiles at level y% weighted by the median:

$$X_{y\%} = \frac{x^{+}_{y\%} - x^{-}_{y\%}}{x_{\text{median}}} \quad (6)$$

where, $x^{+}_{y\%}$ is the y-th percentile of the samples in the quantity vector x of which values are exceeding the median of the vector itself, and $x^{-}_{y\%}$ is the complementary percentile, that corresponds to the (100 – y-th) percentile. This difference measures the amount of samples lying in the central part of the signal, within the boundary set by the y% value. The y-th percentile displacement factor $\xi_{y\%}$ is then defined as the ratio of the two complementary y-th percentiles considered above:

$$\xi_{y\%} = \frac{x^{+}_{y\%}}{x^{-}_{y\%}} \quad (7)$$

F. Band-pass filter

The band-pass filter index y_{bp} was proposed in [6] to overcome the computational complexity of (4). The preferred implementation is an IIR filter (Butterworth), compared to FIR and considering the demanding requirement of the 1 Hz cutoff. It is important to separate the low-frequency content featuring voltage fluctuations that unavoidably would fall inside the ripple calculation. The high-frequency cutoff conversely defines the maximum frequency tracked by the algorithm, and thus which faster transients will be rejected. This cutoff frequency may suit thus regulatory frequency intervals, such as 2/3.6 kHz for harmonics, and 150 kHz for conducted emissions. Tests are done with a cut-off frequency of 1 and 5 kHz, following the implementation in [6].

III. PQ INDEXES BEHAVIOR AND PERFORMANCE

The indexes considered above have been tested with line voltage recordings of a DC 3 kV railway sampled at 50 kSa/s. The scalar values of the indexes are calculated for each record extracted from the two line voltage recordings shown in Fig. 1; the outputs are characterized by calculating the percentiles with three thresholds (80%, 95% and 99%) and the value of the maximum.

The DFT used for *LFSD*, q_{SA} and q_{SAP}, is calculated over a 1 s time window, used then also for the other indexes. A total of 1700 records were collected.

The test signals tst06 and tst14 are first benchmarked with basic spectral analysis (windowed DFT in Fig. 2) and standard robust statistics, such as Mean Absolute Deviation, Geometric Mean, Skewness and Kurtosis, whose results are shown in Table 1.

Table 1. Robust statistics for tst06 and tst14

	test06	test14a	test14all
Geometric mean	3701.2 V	3421.2 V	3427.2 V
Mean abs. dev.	56.20 V	47.15 V	62.07 V
Skewness	-0.426	0.4045	1.552
Kurtosis	3.173	2.897	6.275

Note: “test14a” indicates line voltage samples cut before the step change; “test14all” includes all samples of tst14.

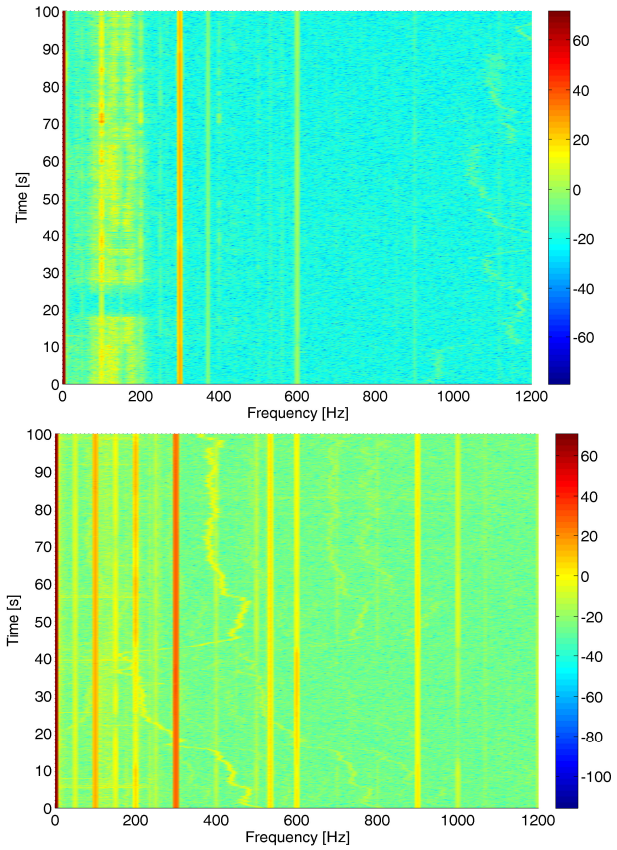

Fig. 1. Spectra of the test signals: (top) tst06, (bottom) tst14

Although spectrally speaking (see Fig. 2) *tst06* has higher low-frequency non-characteristic components, its statistics are better compared to *tst14all* (that includes the step change) and comparable excluding it. The ripple is mainly caused by the three strongest rectifier harmonics: 300 Hz (6th), 600 Hz (12th) and 100 Hz (2nd).

The negative Skewness of *tsts06* indicates a “tail” on the left, visible from its plot; in general distributions are asymmetric, but we will see that 20%, 5% and 1% percentiles show little asymmetry, indicating thus that the skewness is in around the mean, caused by fluctuations and not spikes. The Kurtosis is quite large, similar or worse than a Normal distribution (*ku*=3).

The statistic results are shown in Table 2 and 3.

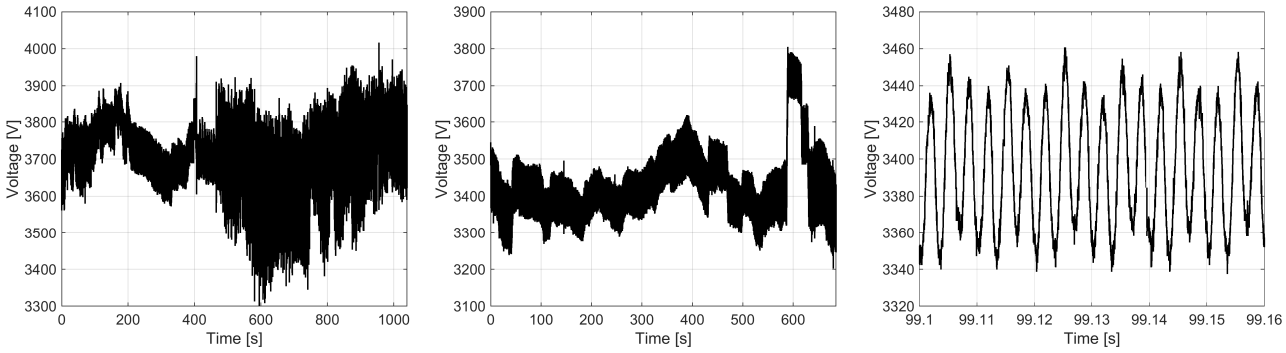

Fig. 2. Example of DC line voltage record used for comparison: (left & middle) two traces, test06 and test14, with quite different line voltage profile; (right) zoom with the 300 Hz main ripple and the 100 Hz modulation (visible in peaks stacked 3-by-3)

Table 2. Percentiles for tst06 and tst14 of the band-pass and DFT implementations: BP, SA, SAP [6][7]

		test06	test14a	test14all
$y_{bp,\mathrm{BU}/1\text{-}1\mathrm{kHz}}$	pct. 80%	3732.0 V	3420.4 V	3464.5 V
	pct. 95%	3765.2 V	3438.3 V	3481.0 V
	pct. 99%	3807.3 V	3450.1 V	3488.0 V
	max	**3960.1 V**	**3519.1 V**	**3522.1 V**
$y_{bp,\mathrm{BU}/1\text{-}5\mathrm{kHz}}$	pct. 80%	3732.1 V	3420.4 V	3481.8 V
	pct. 95%	3765.4 V	3438.4 V	3501.2 V
	pct. 99%	3807.5 V	3450.5 V	3523.1 V
	max	**3965.1 V**	**3530.0 V**	**3532.4 V**
$q_{SA/1\text{-}1\mathrm{kHz}}$	pct. 80%	3775.3 V	3460.9 V	3482.3 V
	pct. 95%	3799.3 V	3470.4 V	3491.7 V
	pct. 99%	3815.8 V	3485.1 V	3507.2 V
	max	**3845.0 V**	**3492.3 V**	**3514.9 V**
$q_{SAP/1\text{-}1\mathrm{kHz}}$	pct. 80%	3722.4 V	3450.3 V	3472.3 V
	pct. 95%	3733.7 V	3461.3 V	3482.6 V
	pct. 99%	3745.2 V	3471.5 V	3493.7 V
	max	**3768.2 V**	**3479.9 V**	**3502.5 V**
$q_{SA/1\text{-}5\mathrm{kHz}}$	pct. 80%	3776.0 V	3461.1 V	3482.5 V
	pct. 95%	3799.3 V	3470.4 V	3491.9 V
	pct. 99%	3815.8 V	3485.1 V	3507.2 V
	max	**3845.0 V**	**3492.3 V**	**3514.9 V**
$q_{SAP/1\text{-}5\mathrm{kHz}}$	pct. 80%	3722.3 V	3450.3 V	3472.3 V
	pct. 95%	3733.7 V	3461.3 V	3482.6 V
	pct. 99%	3745.2 V	3471.5 V	3493.7 V
	max	**3768.2 V**	**3479.9 V**	**3502.5 V**

Table 3. Percentiles for tst06 and tst14 of the base-band percentiles implementation [9]

		test06	test14a	test14all
$x^{+}_{y\%}$	pct. 80%	3763.4 V	3424.1 V	3522.9 V
	pct. 95%	3812.3 V	3455.8 V	3686.5 V
	pct. 99%	3846.4 V	3482.7 V	3734.1 V
$x^{-}_{y\%}$	pct. 80%	3647.5 V	3355.7 V	3365.5 V
	pct. 95%	3573.0 V	3315.4 V	3321.5 V
	pct. 99%	3516.8 V	3289.8 V	3292.2 V
$X_{y\%}$	pct. 80%	0.0313	0.0202	0.0460
	pct. 95%	0.0645	0.0414	0.1067
	pct. 99%	0.0888	0.0569	0.1292
$\xi_{y\%}$	pct. 80%	1.0318	1.0204	1.0468
	pct. 95%	1.0670	1.0423	1.1099
	pct. 99%	1.0937	1.0586	1.1342

Considering the band-pass filter algorithm tested in Table 2, the mean value of the signal was added to the filter pure ac output of the band-pass filter, to be able to compare it to the other indexes: the result is almost unchanged when the upper corner frequency is moved from 1 kHz to 5 kHz; the reason is the lack of significant high-frequency harmonics in the two signals.

The results based on DFT for SA and SAP do not change when the bandwidth is brought from 1 to 5 kHz. The calculation of the DFT is done with 1 Hz resolution to include 1 Hz as minimum frequency, for a fair comparison with the other indexes. However, the DFT components are pruned using a 1% threshold to remove the noise floor, thing that is not possible with the band-pass filter implementation. From this the largest values obtained from y_{bp} compared to SA and SAP: the difference is however limited to about 2%, in line with the applied threshold. As already noted [6], SA based on absolute values gives always larger values than SAP, because there is no compensation between components that form the ripple and they are always added in phase (arithmetic composition).

For the set of percentiles in Table 3, the parameter $X_{y\%}$ shows to be sensitive to the step change in *tst14*, more than doubling its value; the ratio $\xi_{y\%}$ is less sensitive and changes only by few %.

The band-pass filter gives values smaller than those obtained with the percentiles: the difference is smaller for *tst06* (about 1-2%) and larger for *tst14*, due to the presence in the latter of the voltage step change; the voltage step is almost rejected using the band-pass filter that has a minimum frequency of 1 Hz.

Robust statistics are probably more effective in general to characterize signal changes; the use of percentiles and other similar statistical estimates should be thus analyzed further, identifying which combinations describe better the signal characteristics, backing up their weakness (the lack of a band definition) by the simplest and most straightforward techniques as possible (wavelets [14][15], Empirical Mode Decomposition [17][19] and band-pass IIR filters [6], in order of decreasing complexity and computational load).

IV. CONCLUSIONS

This work is a preliminary assessment of the performances and peculiarities of DC PQ metrics proposed in the literature in the last twelve years.

The indexes based on DFT, on band-pass filtering and percentiles show a significant agreement, although each weights differently some signal characteristics. This is a starting point for the equivalence of three indexes based on different approaches.

The considered indexes can in principle be extended beyond the usual 2-3 kHz limit used for PQ analysis of AC systems (for phenomena as the so-called harmonics and inter-harmonics), covering an extended frequency interval up to 150 kHz (sometimes named "supra-harmonics"), where more complex switching by-products of modern Switched-Mode Power Supplies can be found [17]. For a compact implementation leading to a less computationally intensive analysis, besides the use of fast DFT implementations, filter banks, Empirical Mode Decomposition and wavelet bases may be considered. The approach would be that of splitting the frequency range in sub-intervals, losing the detail of the single

component, but capturing the sub-banded signal power; for emissions assessment approaches based on sub-banded spectra are not only acceptable, but practical, since coupling and interference mechanisms do not take place at narrow frequency intervals, reduced to one or few bins, but in general spread over several bins, from which the grouping of harmonic and inter-harmonic components required by the EN 61000-4-7 [1].

The use of statistical quantities, such as mean, dispersion and percentiles, or histograms, is a powerful tool to describe the behavior and the distribution of amplitude once the signal has been split into sub-bands.

Future developments will be in the direction of applying and assessing wavelets and Empirical Mode Decomposition, comparing them especially with a simple and straightforward implementation as the band-pass filter.

V. ACKNOWLEDGMENT

The results here presented are developed in the framework of the 16ENG04 MyRailS Project and European Union's Horizon 2020 research and innovation program. This work was supported by the Swiss State Secretariat for Education, Research and Innovation (SERI) under contract number 17.00127. The opinions expressed and arguments employed herein do not necessarily reflect the official views of the Swiss Government.

REFERENCES

[1] EN 61000-4-7, *Electromagnetic compatibility (EMC) – Part 4-7: Testing and measurement techniques – General guide on harmonics and interharmonics measurements and instrumentation, for power supply systems and equipment connected thereto*, 2009.

[2] EN 61000-4-30, *Electromagnetic compatibility (EMC) – Part 4-30: Testing and measurement techniques – Power quality measurement methods*, 2015.

[3] IEEE Std. 1459, *IEEE Standard Definitions for the Measurement of Electric Power Quantities under Sinusoidal, Nonsinusoidal, Balanced, or Unbalanced Condition*, 2010.

[4] G.T. Heydt and W.T. Jewell, "Pitfalls of electric power quality indices," *IEEE Trans. on Pow. Del.*, vol. 13, no. 2, Apr. 1998, pp. 570-578.

[5] M. Caserza Magro, A. Mariscotti, P. Pinceti, "Definition of Power Quality Indices for DC Low Voltage Distribution Networks", IEEE Intern. Meas. Techn. Conf. IMTC, Sorrento, Italy, April 20-23, 2006.

[6] A. Mariscotti, "Methods for Ripple Index evaluation in DC Low Voltage Distribution Networks", IEEE Intern. Meas. Techn. Conf. IMTC, Warsaw, Poland, May 2-4, 2007.

[7] A. Mariscotti, "DC railway line voltage ripple for periodic and aperiodic phenomena", Intern. Measurement Conference Imeko, Natal, RN, Brazil, Sept. 27-30, 2011.

[8] A. Mariscotti, "Characterization of Power Quality transient phenomena of DC railway traction supply", *ACTA IMEKO*, July 2012, Vol. 1, n. 1, pp. 26-35.

[9] I. Ciornei, L. Hadjidemetriou, M. Albu, E. Kyriakides and M. Sanduleac, "Analytical derivation of PQ indicators compatible with control strategies for DC microgrids", IEEE PES PowerTech, June 2017, Manchester, UK.

[10] MIL-STD-704F, *Aircraft electric power characteristics*, March 2004.

[11] J. Barros, M. De Apráiz and R. I. Diego, "Definition and Measurement of Power Quality Indices in Low Voltage DC Networks", IEEE 9th Intern. Workshop on Applied Meas. for Power Sys. (AMPS), Sept. 26-28, 2018, Bologna, Italy.

[12] J. Barros, M. De Apráiz, R.I. Diego, "Power Quality in DC Distribution Networks," *Energies*, vol. 12, no. 5, 2019, pp. 848.

[13] E. A. Larsson *et al.*, "Measurements of high-frequency (2-150 kHz) distortion in Low-Voltage networks," *IEEE Trans. on Power Delivery*, vol. 25, no. 3, pp. 1749-1757, July 2010.

[14] L. Angrisani *et al.*, "A Measurement Method based on the Wavelet Transform for Power Quality Analysis," *IEEE Trans. on Pow. Del.*, vol. 13, no. 4, pp. 990-998, Oct. 1998.

[15] J. Barros and R.I. Diego, "Analysis of Harmonics in Power Systems Using the Wavelet-Packet Transform," *IEEE Trans. on Instrum. and Meas.*, vol. 57, no. 1, Jan. 2008, pp. 63-69.

[16] T. Lin and A. Domijan, "On Power Quality Indices and Real-Time Measurement", *IEEE Trans. on Power Delivery*, vol. 20, n. 4, Oct. 2005, pp. 2552-2562.

[17] L. Sandrolini and A. Mariscotti, "Techniques for the Analysis of Time-Domain Conducted Emissions of SMPS in Smart Grids", 19th Intern. Conf. on Environmental and Electrical Engineering, June 11-14, 2019, Genova, Italy.

[18] EN 61000-4-19, *Electromagnetic compatibility (EMC) - Part 4-19: Testing and measurement techniques - test for immunity to conducted, differential mode disturbances and signalling in the frequency range 2 kHz to 150 kHz at a.c. power ports*, CENELEC, 2014.

[19] N. E. Huang, Z. Shen, S. Long, M. Wu, H. Shih, Q. Zheng, N.-C. Yen, C. Tung, and H. Liu, "The empirical mode decomposition and the Hilbert spectrum for nonlinear and non-stationary time series analysis," *Proc. R. Soc. Lond.* A454, pp. 903–995, March 1998.